International Journal of Engineering Science Invention (IJESI)
ISSN (Online): 2319-6734, ISSN (Print): 2319-6726
www.ijesi.org ||Volume 11 Issue 1 Series I || January 2022 || PP 01-14

Characterization of microgranular enclaves of Hyderabad batholith, Eastern Dharwar Craton, India.

[1]S Ramesh, [1]Ch Narshimha and [1]U.V.B. Reddy
[1]*Department of Applied Geochemistry, Osmania University, Hyderabad-500 007, India*

Abstract
Microgranular enclaves (ME) in Neoarchean granites of Hyderabad Batholith, Eastern Dharwar Craton (EDC) studied for their field relationships, petrographic and geochemical characteristics and evaluated their petrogenesis. The ME are fine grained, melanocratic to mesocratic, phenocryst free enclaves with rounded, sub-rounded, elongated shapes with various sizes. The sharp to gradational contact with wisp tails and transitional diffuse boundaries evidences that ME magma had interacted with the host granite during the crystallization suggesting liquid– liquid interaction. MEs grading into schlieren may be related to chaotic dynamics involving mafic and silicic magmas whose viscosities are close to each other. The occurrence of syn- plutonic mafic dykes with near completely mixed zone, cuspate contact, and magmatic flow textures, suggest the coeval emplacement of felsic and mafic end- member magmas. Whole- rock geochemical data indicates MEs have low SiO_2 and high total alkalies, high MgO, Al_2O_3, Fe_2O_3, CaO and Na_2O contents with enriched compatible elements, relatively high Ni, Cr, and Co. MEs are calc-alkaline, metaluminous occupying in the field of trachyandesite-basaltic trachyandesite-basaltic andesite to basaltic field. In the chondrite-normalized REE patterns, MEs are indistinguishable with highly enriched LREE and depleted HREE patterns and negative Eu anomalies.

Date of Submission: 10-01-2022 Date of Acceptance: 25-01-2022

I. INTRODUCTION

Microgranular Enclaves (ME) are most important diagnostic rock fragments enclosed in many granitoids. They occur in host rock because of different magmatic possesses and provide significant insight into the understanding of operative physical and chemical processes during evolution of granite magmatic systems (Kumar et al., 2020; Kumar, 2020; Kumar et al., 2017a; Clemens et al. 2016; Kumar 1995, 2010, 2014; Kumar et al. 2004; Kumar & Rino 2006; Perugini et al. 2007; Didier & Barbarin, 1991; Vernon, 1984; Wiebe, 1994; Didier, 1973). ME provides vital clues on evolution of granitic magmas and the dynamics of magma chamber processes. Mafic magmatic enclaves (MME) are more mafic than their host rocks occur as products of uncompleted mixing between coeval mafic and felsic magmas and provide much insight in understanding the magma chamber processes, chemical diversity and accretinary history of calc-alkaline batholiths.

Archean cratons all over the world contains voluminous Tonalite-Tronjhemite-Granodiorite, calc-alkaline to potassic plutons (Jayananda et al., 2014). Neoarchean granites of EDC are encompassing most of the craton with a sparse remnant of older TTG rocks. The EDC formation, its reworking and tectonomagmatic processes are explained through plume-arc accretion and cratonization (Manikyamba et al. 2004a, b, 2009; Smithies et al. 2009; Manikyamba and Kerrich 2012; Barnes and Van Kranendonk 2014). The calc-alkaline to potassic plutons are the most voluminous lithologies in the EDC and form a wide window for magma chamber processes at different crustal levels (Jayananda et al., 2014). The genesis of granitic batholiths are highly debatable in terms of melt accumulation, source, hybridization, metasomatism and tectonic emplacement. As per Huppert and Sparks (1988) the lower crustal remelting of thick older TTG gneisses is responsible for the growth of granitic batholiths through assimilation and fractional crystallization, which are the dominant magmatic processes for which the basaltic magmatism acted as a heat source.

The Hyderabad Granite Batholith (HGB) in the northeastern part of EDC is a vast granitic terrain is a combination of a variety of granitoids such as aplites, granites, granodiorites, monzogranites, syenogranites, alaskites, etc. (Pahari et al. 2020; Narshimha et al. 2020; Pahari et al. 2019; Anjaneyulu et al. 2019; Praveen et al. 2018). Jayananda et al. (2014), Shukla and Ram Mohan (2019) studied the Neoarchean granites and associated MME from the Nalgonda region and suggested magma mixing processes in the genesis of the host granite with differences in the degree of dilution of mafic magma and diffusive fractionation processes in a subduction zone environment. Present study deals with the detailed field relationships, petrography and geochemical characteristics of ME occurring in Hyderabad granites of HGB, Eastern Dharwar Craton in order to understand the genesis and their role in the evolution of Hyderabad Batholith.

II. REGIONAL GEOLOGY

The Dharwar Craton (DC) is one of the large and oldest cratons in peninsular India, bounded by Eastern Ghats Granulite Belt (EGGB) in the east, Southern Granulite Terrain in the south and Proterozoic platform basins in the north (Ramakrishnan and Swaminath 1981). DC has prolonged evolution history from 3.6 to 2.5 billion years (Chardon et al., 2011). The craton consists of Tonalite-Trondhjemite Granodiorite (TTG) gneisses also called as peninsular gneisses, older Sargur greenstones, younger Dharwars and 3.0 to 2.5 Ga felsic plutonic rocks with calc-alkaline to potassium rich nature. DC can be divided into Eastern Dharwar Craton (EDC) and Western Dharwar Craton (WDC) by the mylonitic shear zone that is adjacent to the Chitradurga belt. This division is based on mainly thickness of the craton, composed rocks and structural features (Swaminath et al., 1976; Chadwick 2000; Chardon et al., 2008, 2011; Jayananda et al., 2006; Manikyamba et al. 2017).

The EDC comprises Neoarchean greenstone belts, TTG gneisses, transitional TTGs, high Mg granitoids and 2.5 Ga younger potassic anatectic granites with sporadic occurrence of the older peninsular gneisses (Balakrishnan et al. 1999; Krogstad et al. 1991; Peucat et al. 1993; Jayananda et al. 1995, 2000; Chadwick et al. 2000; Sarvothaman 2001; Moyen et al. 2001, 2003; Chardon and Jayananda 2008; Dey et al. 2014; Nandy et al. 2019). The granitoid magmatism in the northwestern part of the EDC initiated at 2.68 Ga with gneissic granodiorites of intermediate composition between sanukitoid and TTG. This was followed by intrusion of 2.5 Ga transitional TTGs. The sanukitoid to Closepet type magmatism with the intrusion of K-rich leucogranites mark the cratonization at 2.53–2.52 Ga.

The granites from Hyderabad region are confined to Precambrian younger gneissic complex in the northeastern part of eastern Dharwar Craton, bounded by Karimnagar granulite belt and Godavari Graben in the northeast, Proterozoic Cuddapah basin in the south and Deccan Traps in the northwest (Figure 1a&b). The Gadwal, Peddavuru, Ghanapur, Yerraballi greenstone belts and sedimentary rocks of Mulugu sub-basin of Pakhal Supergroup are located alongside of the Hyderabad batholith. This composite batholith has discrete root extending to a depth of more than 10 km covering an area of 10000 km2, consisting of several criss-cross major and minor lineaments, pre-existing faults which are responsible for vertical adjustments and Neotectonic activity (Pandey et al. 2002; Singh et al. 2004). ENE–WSW and NNW–SSE maBc dykes are widespread throughout this batholith (Murthy 1995; Radhakrishna et al. 2004)

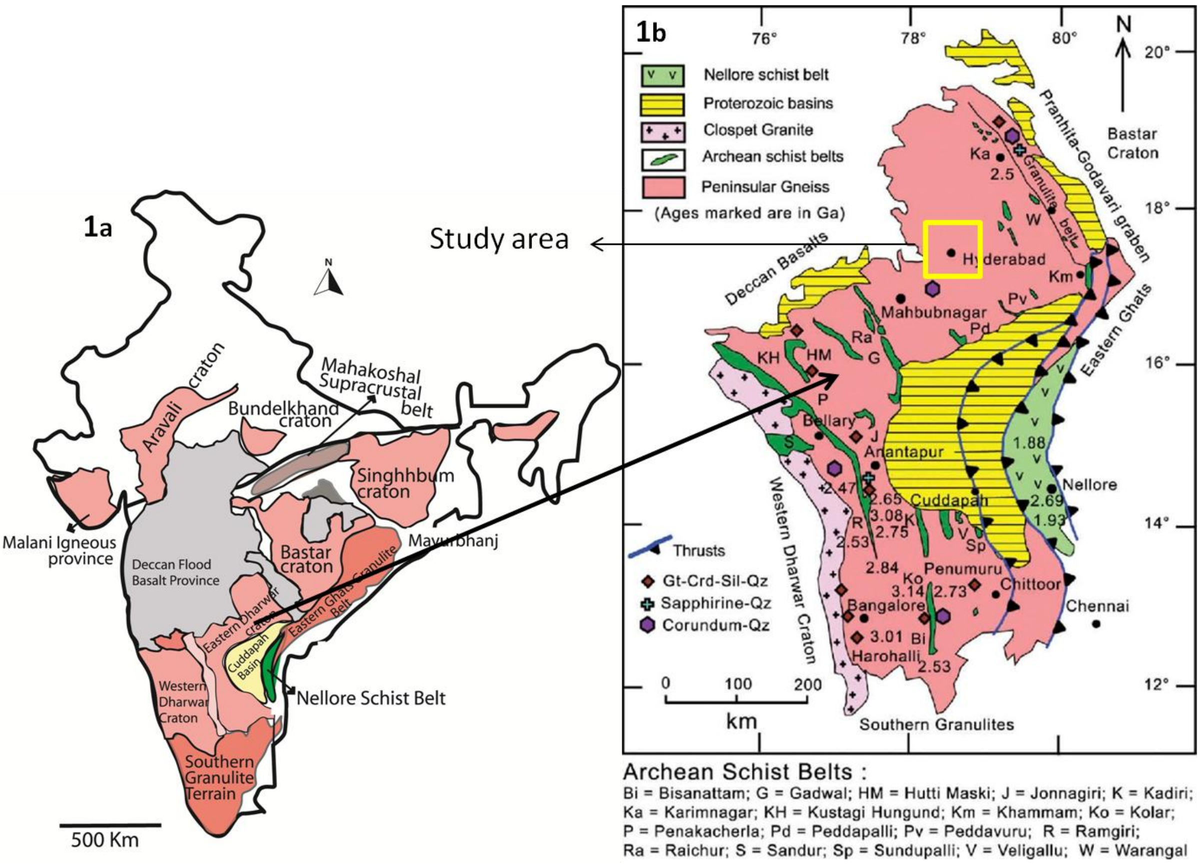

Fig.1 Geological map of the Eastern Dharwar Craton showing the distribution of various litho units (after Naqvi and Rogers, 1987).

III. FIELD RELATIONSHIPS AND PETROGRAPHY

Microgranular enclaves in HGB exposed around the Hyderabad city are investigated for this study. The host Granitic rocks are generally massive, medium to coarse grained, equigranular to inequigranular, K-feldspar rich pink to plagioclase rich grey type rock with wide textural variations. These rocks show occasionally foliated features. These granite rocks show wide range of color index from leucocratic to light light grey to grayish pink and some biotite rich rocks are mesocratic in color. The petrographic study of these rocks exhibits equigranular and hypidiomorphic granular texture**.** The rocks in the study area are classified as syenogranite, monzogranite and granodiorite based on the modal % of quartz, alkali feldspar and plagioclase**.**

The MEs are melanocratic and mesocratic, fine-grained, equigranular, phenocryst free enclaves with rounded, sub-rounded, elongated shapes with various sizes. Field observations suggest that numerous melanocratic disintegrated syn- plutonic mafic dyke with varied widths are found within the granite (Fig. 2a). The abundant occurrence of MEs in vicinity to the synplutonic dyke is an unique feature in these granites. The sharp to gradational contact with wisp tails and transitional diffuse boundaries evidences that ME magma had interacted with the host granite during the crystallization suggesting liquid– liquid interaction (Fig. 2b&c). The extent of mixing is variable, partially mixed and near completely mixed within the host granite.

The MEs are mechanically disintegrated and due fragmented to the intrusion of crystallizing and partly crystallizing felsic magma (Fig. 3a). Subrounded ME mechanically diluting is resulting in spindle structure defines movement of mafic magma within the felsic magma to make interlining contact with host felsic magma (Fig. 3 b&c). Progressive mechanical disaggregation, giving rise the enclaves grading to schlieren of mafic rich composition (Fig. d). These features may be related to chaotic dynamics involving mafic and silicic magmas whose viscosities are close to each other (Barbey et al. 2008; Poli and Perugini, 2002).

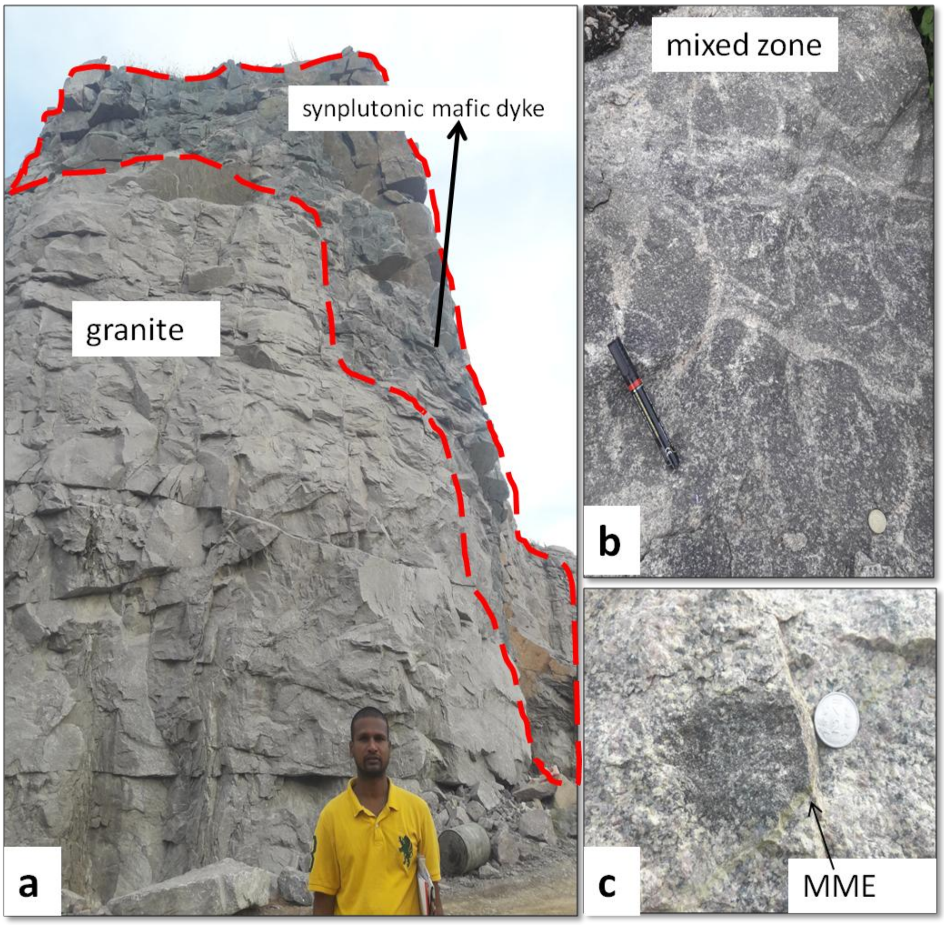

Fig. 2 a) Field photographs illustrating the syn-plutonic mafic dyke within the HGB, b) Depicting near completely mixed zone within the host rock, c) Rounded microgranular enclave within the host rock.

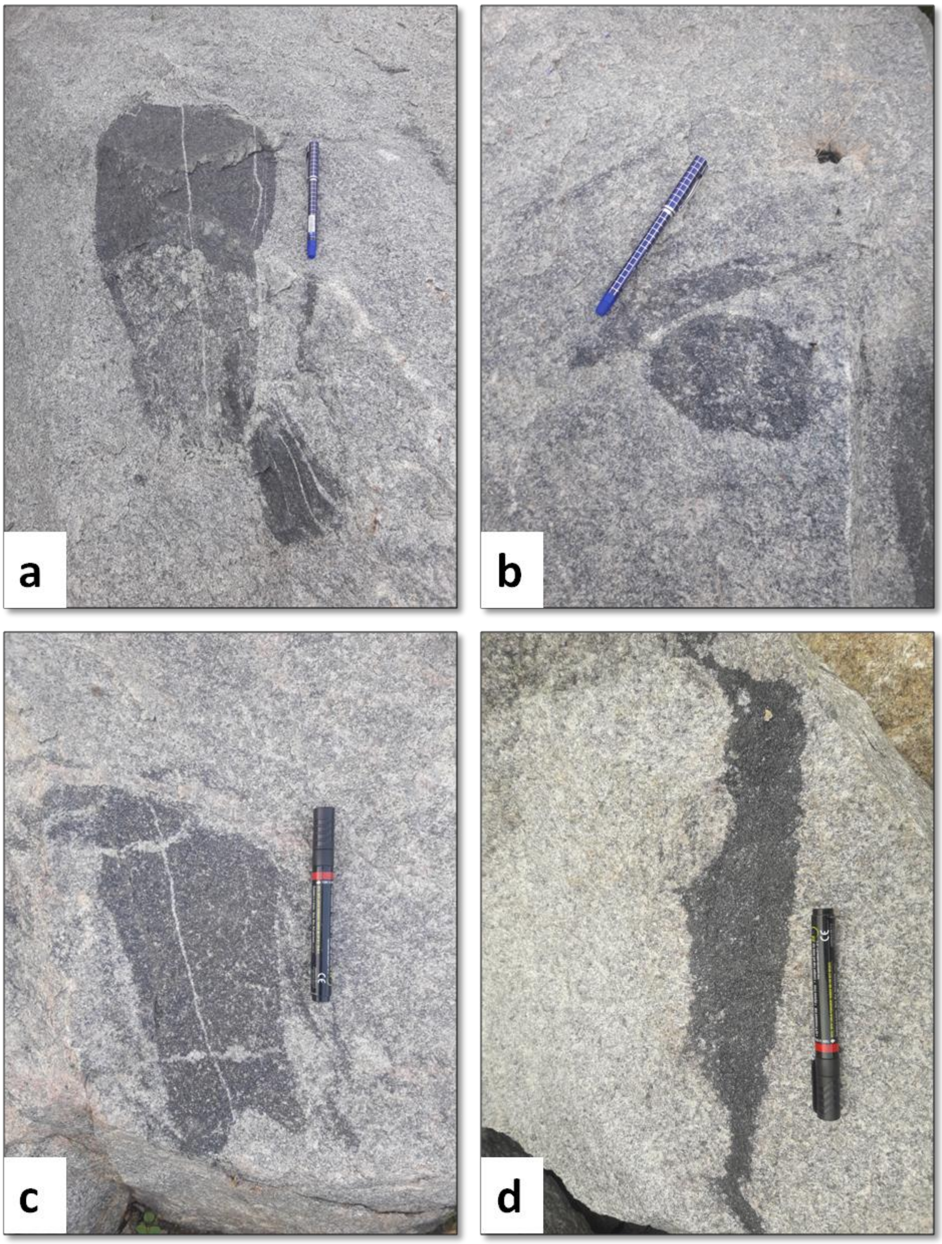

Fig. 3 a) Fine grained mafic microgranular enclave scattered within the host granite, b) ME shows diffused boundary, c) Mafic elongated MEs globule got disintegrated due to intrusion of crystallizing felsic host magma, d) ME grading into biotite schlieren indicates synmagmatic shear zones or disrupted synplutonic dykes.

Petrographically MEs composed mainly of biotite, plagioclase, quartz, orthoclase and amphibole minerals. The accessory minerals are mainly apatite, titanite, zircon and opaques. Biotite is dominating mineral phase and their preferred orientation in ME, defining the flow direction of magma (Fig. 4a). Plagioclase coarse to fine with lammelar twinning occasionally shows dusty appearance and show resorption rim an evidence of disequilibrium result of mixing processes (Fig. 4b). The perthitic and myrmekite intergrowth textures show the sub-solidus recrystallization of feldspars (Fig. 4c). Altered plagioclase and K-feldspar, fine grained clusters of quartz and mafic minerals with nearly rounded grains and opaques with titanite rim are common features (Fig. 4d,e,f,g&h). Titanite corona around opaques (ilmenite?) in ME supports their chemical hybridization with host granite (Nakada, 1991).

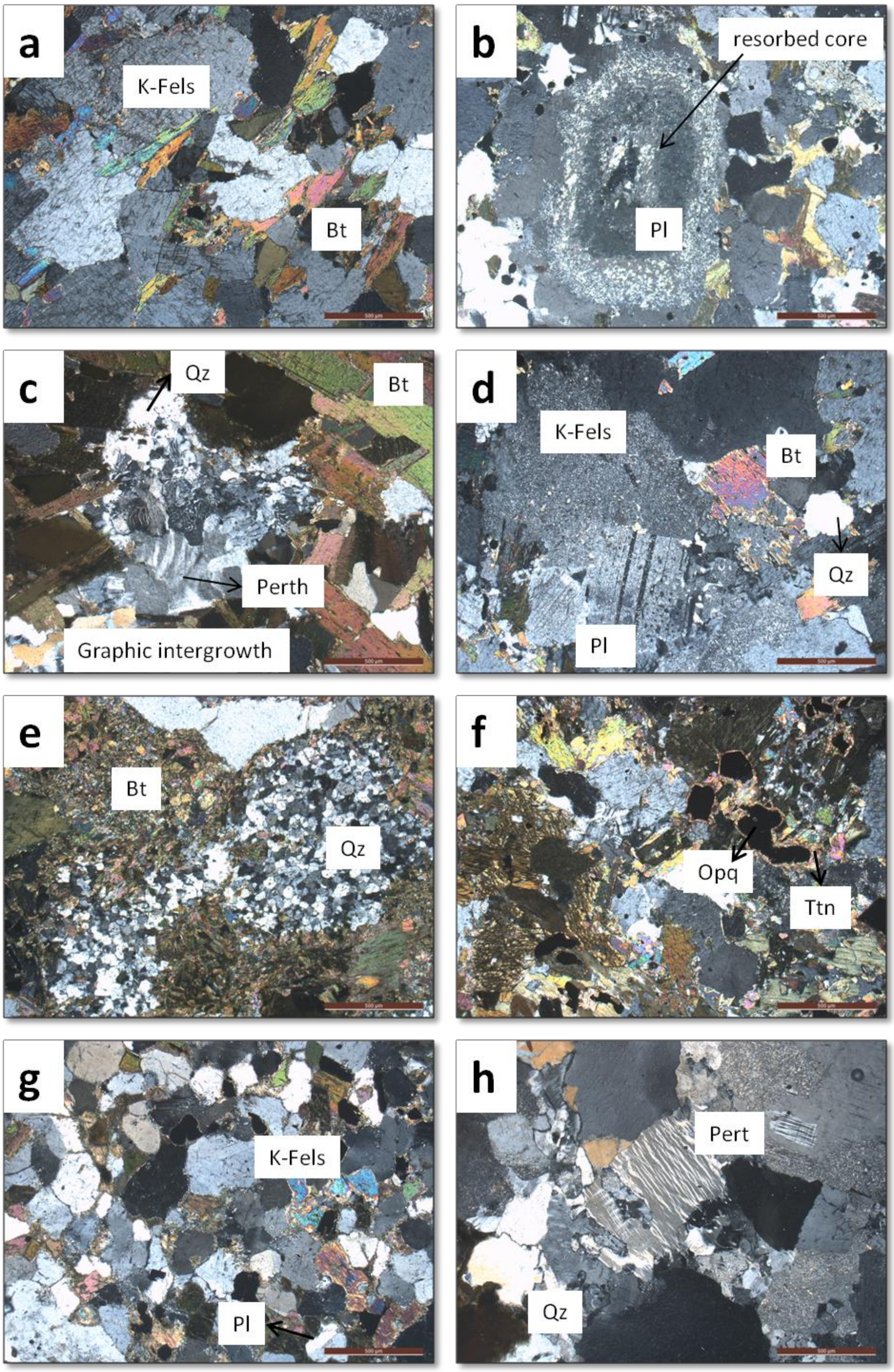

Fig. 4a) Photomicrographs illustrating the preferred orientation of mafic minerals in ME, defining the flow direction,, b) Plagioclase within ME showing a resorption rim an evidence of disequilibrium, c) Graphic intergrowth of alkali feldspar and quartz in ME, d) Altered K-feldspar and plagioclase with biotite inclusions, e) Quartz and biotite clusters within ME, f) Fine grained titanite corona around opaques, g) K-feldspar, quartz, plagioclase and biotite minerals in ME with nearly rounded grains, h) Intergrowth of perthite.

IV. GEOCHEMISTRY

A total of 21 ME samples collected from the HGB. Whole rock geochemistry includes major, minor and trace element abundances were determined by XRF and HR-ICP-MS Lab, Geochemistry Division, CSIR-National Geophysical Research Institute, NGRI Hyderabad. The geochemical data of representative samples were presented in Table 1.

ME have low silica content ranging from 45.42 to 53.58 wt.% with an average 50.58 wt%, high MgO from 2.48 to 10.74 wt%. with an average 7.54 wt%. and CaO is ranging from 3.6 to 7.06 with an average 5.83. The ME are characterized by high total alkalies (average 9.02 wt%) and moderate to high aluminium content (9.10–13.08 wt.% with an average of 11.41wt%). Fe_2O_3 content ranges from 11.02 wt% to 12.99 wt% with an average is 12.30 wt%. Generally the MEs are enriched in compatible elements like CaO, MgO and Fe_2O_3. In the Harker diagrams, MEs show linear trends, with decreasing MgO, K_2O, Al_2O_3, TiO_2, P_2O_5, A/CNK, Y, Zr, La and Ce and increasing Na_2O, CaO, FeO, Cr, and Ba relative to SiO2 (Fig. 5 - 6).

Trace element geochemistry indicates that the ME consists of relatively high Ni (26 to 490 ppm), Cr (73 to 1602 ppm), and Co (5.8 to 62.6 ppm). The high field strength element contents in ME show moderate abundances. Total-alkali silica (TAS) diagram (Le Maitre, 2002) evidences that ME are alkaline occupying in the field of trachyandesite-basaltic trachyandesite-basaltic andesite to basaltic field (Fig. 7a).The A (Na_2O+K_2O, F (Fe^T) M (MgO) plot after Irvine & Baragar (1971) shows the calc-alkaline affinity of the MEs (7b). MEs in the alumina saturation diagram (Shand, 1943) fall in the metaluminous field, while a few samples fall close to the boundary of peralkaline field (Fig. 7c).In the chondrite-normalized REE patterns, ME are indistinguishable with highly enriched LREE and depleted HREE patterns and negative Eu anomalies (Fig. 8a). Primitive mantle normalized (normalizing values after Sun and McDonough, 1989) multielement diagram (Fig. 8b) of the ME shows prominent negative anomalies in Ba, Nb, Sr, P, Zr, Eu, and Ti, while Th, U, Ce, Pr, Nb, Sm, Dy, Y, and Nd show positive anomalies.

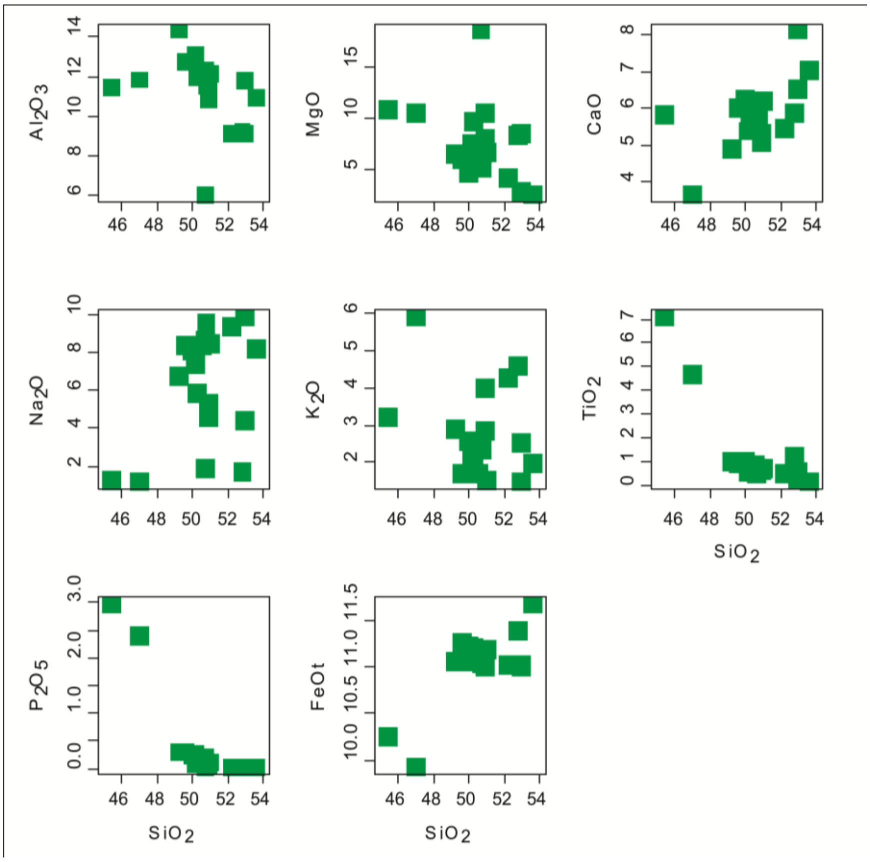

Fig.5. Plots of SiO_2 versus major oxides variation diagram of MEs show different trends

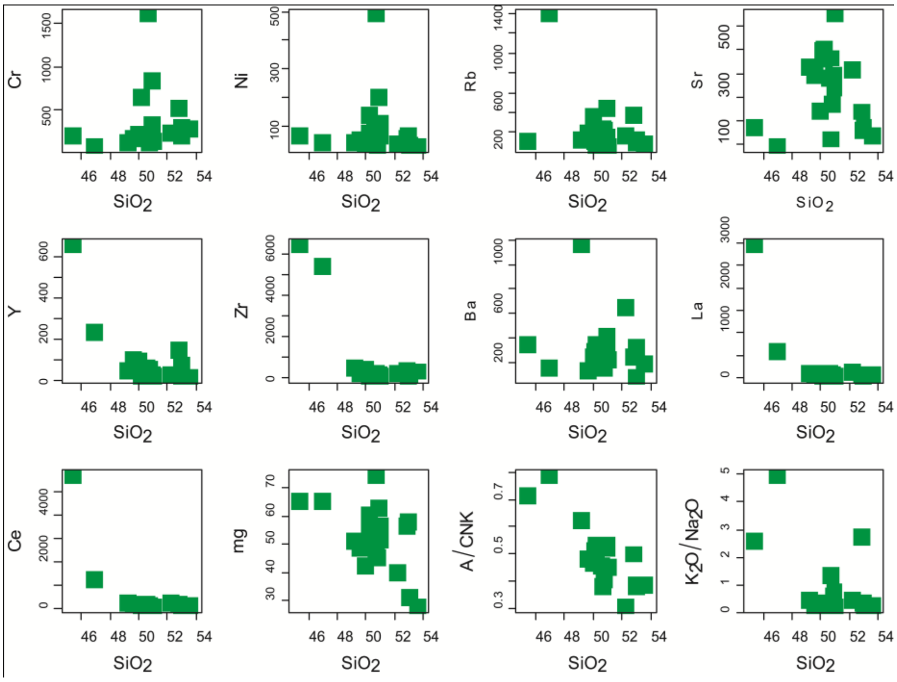

Fig.6. Plots of SiO_2 (wt%) versus Trace elements (ppm) variation diagram of MEs show different trends.

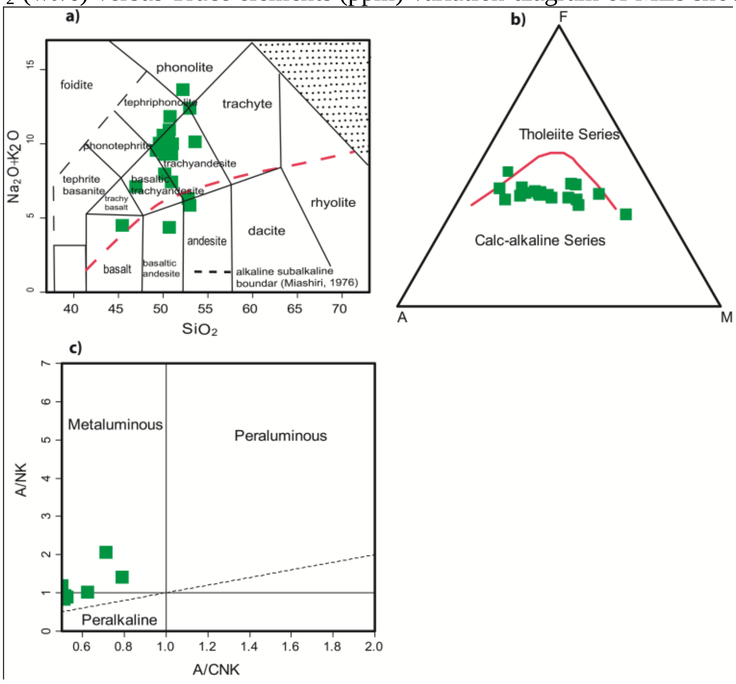

Fig.7. a) Total-alkali (Na_2O+K_2O wt.%) vs. SiO_2 (TAS) diagram (Le Maitre, 2002) wherein ME samples are occupies in the field of trachyandesite-basaltic trachyandesite-basaltic andesite to basalt, b) AFM diagram for ME shows their calc-alkaline nature, c) Alumina saturation index diagram A/NK vs. A/CNK (Shand, 1947; Maniar and Piccoli, 1989) for ME.

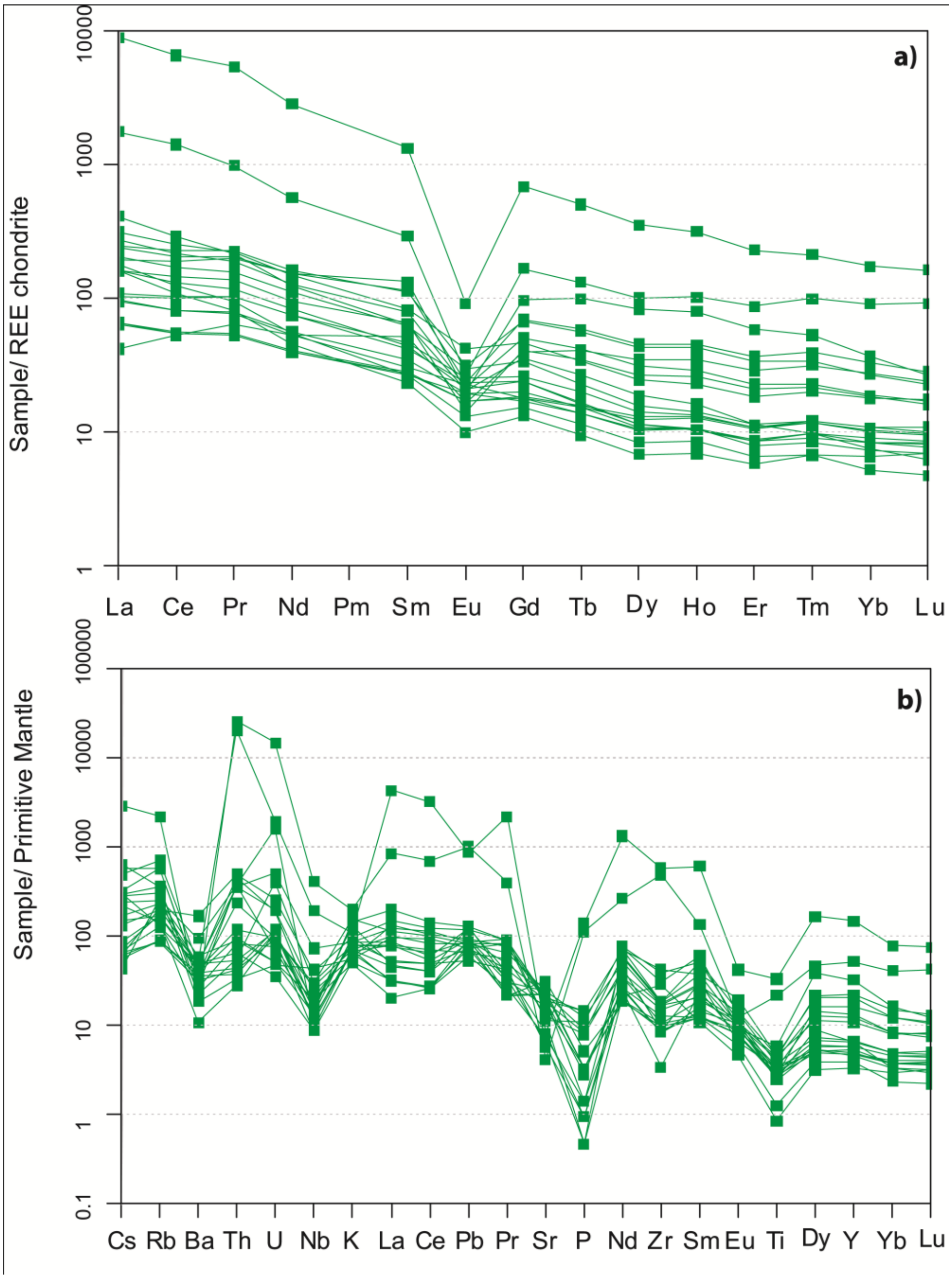

Fig.8. a) Chondrite-normalized REE patterns and b) primitive mantle normalized (values after Sun and Mc Donough,1989) multi element diagrams of MEs.

V. CONCLUSIONS

Microgranular Enclaves of Hyderabad granites are fine grained, meso-melanocratic with igneous textures formed in rounded, sub-rounded, elongated shapes and various sizes. Field and textural features evidences that ME magma had interacted with the host granite during the crystallization suggesting liquid–liquid interaction. The two end members of mafic (ME) and silicic (host) magma viscosities are likely close to each other. The occurrence of syn- plutonic mafic dykes with near completely mixed zone, cuspate contact, and magmatic flow textures, suggest the coeval emplacement of ME and host granite. Geochemically, MEs are calc-alkaline, metaluminous occupying in the field of trachyandesite-basaltic trachyandesite-basaltic andesite to basaltic field. It appears that coeval basaltic magmas intruded into crystallizing granite magma. Chemical mixing between two magma end-members in various proportions probably produced the MEs in Hyderabad granite batholith.

ACKNOWLEDGEMENTS

The authors are grateful to the Head Department of Applied Geochemistry, Osmania University, Hyderabad for encouragement and the Director, CSIR-National Geophysical Research Institute, Hyderabad, for analytical support. First author acknowledges the funding provided by Department of Science & Technology under INSPIRE Fellowship (2014/IF140904).

REFERENCES

[1]. Anjaneyulu M, Nagaraju K and Reddy I P (2019) Petrological and geochemical studies of precambrian granitoids from cherlapally area, Nalgonda district, Telangana state, India; J. Appl. Geochem. 21 311–316.

[2]. Balakrishnan S, Rajamani V and Hanson G N (1999) U–Pb ages for zircon and titanite from the Ramagiri area, southernIndia: Evidence for accretionary origin of the Eastern Dharwar Craton during the late Archean; J. Geol. 107 69–86.

[3]. Barbey P, D. Gasquet, C. Pin, A.L. Bourgeix (2008) Igneous banding, schlieren and mafic enclaves in calc-alkaline granites: The Budduso pluton (Sardinia) Lithos 104 (2008) 147–163. doi:10.1016/j.lithos.2007.12.004

[4]. Barnes S J and Van Kranendonk M J (2014) Archean andesites in the east Yilgarn craton, Australia: Products of plumecrust interaction? Lithosphere 6 80–92.

[5]. Chadwick B, Vasudev V N and Hegde G V (2000) The Dharwar craton, southern India, interpreted as the result of Late Archaean oblique convergence; Precamb. Res. 99 91–111.

[6]. Chardon D and Jayananda M (2008) Three-dimensional Beld perspective on deformation, Cow, and growth of the lower continental crust (Dharwar Craton, India); Tectonics 27 1–15.

[7]. Chardon D, Jayananda M and Peucat J J (2011) Lateral constrictional flow of hot orogenic crust: Insights from the Neoarchean of south India, geological and geophysical implications for orogenic plateaux; Geochem. Geophys. Geosys. 12(2) 1–24.

[8]. Clemens, J.D., Regmi, K., Nicholls, I.A., Weinberg, R. & Maas, R. (2016) The Tynong pluton, its mafic synplutonic sheets and igneous microgranular enclaves: the nature of the mantle connection in I-type granitic magmas. Contributions to Mineralogy and Petrology, 171, 35, https://doi.org/10.1007/s00410-016-1251-y.

[9]. Dey S, Nandy J, Choudhary A K, Liu Y and Zong K (2014) Origin and evolution of granitoids associated with the Kadiri greenstone belt, eastern Dharwar craton: a history of orogenic to anorogenic magmatism; Precamb. Res. 246 64–90.

[10]. Didier J and Barbarin B (eds) (1991) Enclaves and Granite Petrology Developments in Petrology. Amsterdam: Elsevier, 625.

[11]. Didier, J. (1973) Granites and their enclaves: The Bearing of Enclaves on the Origin of Granites. Developments in Petrology, v. 3, Elsevier, Amsterdam, 393p.

[12]. Huppert H E and Sparks R S J (1988) The generation of granitic magmas by intrusion of basalt into continental crust; J. Petrol. 29 599–624

[13]. Jayananda M, Chardon D, Peucat J J and Capdevila R (2006) 2.61 Ga potassic granites and crustal reworking in the western Dharwar craton, southern India: Tectonic, geochronologic and geochemical constraints; Precamb. Res. 150 1–26.

[14]. Jayananda M, Gireesh R, Sekhamo K-U and Miyazaki T (2014) Coeval felsic and Mafic Magmas in neoarchean calcalkaline magmatic arcs, Dharwar craton, Southern India: Field and petrographic evidence from mafic to Hybrid magmatic enclaves and synplutonic Mafic dykes; J. Geol. Soc. India 84(1) 5–28.

[15]. Jayananda M, Martin H, Peucat J J and Mahabaleswar B (1995) Late Archaean crust-mantle interactions: Geochemistry of LREE-enriched mantle derived magmas. Exampleof the Closepet batholith, southern India; Contrib. Mineral.Petrol. 119 314–329.

[16]. Jayananda M, Moyen J F, Martin H, Peucat J J, Auvray Band Mahabaleswar B (2000) Late Archaean (2550–2520 Ma)juvenile magmatism in the Eastern Dharwar craton,southern India: Constraints from geochronology, Nd–Srisotopes and whole rock geochemistry; Precamb. Res. 99225–254.

[17]. Krogstad E J, Hanson G N and Rajamani V (1991) U–Pb ages of zircon and sphene for two gneiss terranes adjacent to the Kolar Schist Belt, South India: evidence for separate crustal evolution histories; J. Geol. 99 801–815.

[18]. Kumar S (1995) Microstructural evidence of magma quenching inferred from enclaves hosted in the Hodruša Granodiorites, Western Carpathians. Geol. Carpath., v.46, pp. 379-382.

[19]. Kumar S (2010) Mafic to hybrid microgranular enclaves in the granitoids of Ladakh batholith, Northwest Higher Himalaya: implications on calc-alkaline magma chamber processes. Journal of the Geological Society of India, 76, 5– 25.

[20]. Kumar S (2014) Magmatic processes: review of some concepts and models. In: Kumar, S. & Singh, R.N. (eds) Modelling of Magmatic and Allied Processes. Springer, Berlin, 1– 22.
[21]. Kumar S (2020) Schedule of Mafic to Hybrid Magma Injections Into Crystallizing Felsic Magma Chambers and Resultant Geometry of Enclaves in Granites: New Field and Petrographic Observations From Ladakh Batholith, Trans-Himalaya, India. Frontiers in Earth Science, v.8, 551097.
[22]. Kumar S and Rino, V (2006) Mineralogy and geochemistry of microgranular enclaves in Palaeoproterozoic Malanjkhand granitoids, Central India: evidences of magma mixing, mingling, and chemical equilibration. Contrib. Mineral. Petrol., v.152, pp.591-609.
[23]. Kumar S, Gupta, Saurabh., Sensarma, Sarajit and Bhutani, Rajneesh. (2020) Proterozoic felsic and mafic magmatism in India: Implications to crustal evolution through crust-mantle interactions. Episodes, 43 (1), 203-230.
[24]. Kumar S, Rino V and A B Paul (2004) Field Evidence of Magma Mixing from Microgranular Enclaves Hosted in Palaeoproterozoic Malanjkhand Granitoids, Central India. Gondwana Research 7 (2), 539-548.
[25]. Kumar, S., Rino, V., Hayasaka, Y., Kimura, K., Raju, S., Terada, K. and Pathak, M., (2017a) Contribution of Columbia and Gondwana Supercontinent assembly- and growth-related magmatism in the evolution of the Meghalaya Plateau and the Mikir Hills, Northeast India: Constraints from U-Pb SHRIMP zircon geochronology and geochemistry. Lithos, v. 277, pp. 356-375.
[26]. Manikyamba C and Kerrich R (2012) Eastern Dharwar Craton, India: Continental lithosphere growth by accretion of diverse plume and arc terranes; Geosci. Frontiers 3 225–240.
[27]. Manikyamba C, Ganguly S, Santosh M and Subramanyam K S V (2017) Volcano-sedimentary and metallogenic records of the Dharwar greenstone terranes, India: window to Archean plate tectonics, continent growth, and mineral endowment; Gondwana Res. 50 38–66.
[28]. Manikyamba C, Kerrich R, Khanna T C, Satyanarayanan M and Krishna A K (2009) Enriched and depleted arc basalts, with Mg-andesites and adakites: a potential paired arc–- back-arc of the 2.6 Ga Hutti greenstone terrane, India; Geochim. Cosmochim. Acta 73 1711–1736.
[29]. Manikyamba C, Kerrich R, Naqvi S M and Mohan M R (2004a) Geochemical systematics of tholeiitic basalts from the 2.7 Ga Ramagiri–Hungund composite greenstone belt, Dharwar craton; Precamb. Res. 134 21–39.
[30]. Manikyamba C, Naqvi S M, Mohan M R and Rao T G (2004b) Gold mineralisation and alteration of Penakacherla schist belt, India, constraints on Archaean subduction and Cuid processes; Ore Geol. Rev. 24 199–227.
[31]. Moyen J F, Martin H, Jayananda M and Auvray B (2003) Late Archaean granites: a typology based on the Dharwar Craton (India); Precamb. Res. 127 103–123.
[32]. Moyen J-F, Martin H and Jayananda M (2001) Multi-elementgeochemical modelling of crust–mantle interactions duringlate-Archaean crustal growth: the Closepet granite (south India); Precamb. Res. 112 87–105.
[33]. Murthy N G K (1995) Proterozoic maBc dykes in southern peninsular India; Geol. Soc. India Memoir 33 81–98.
[34]. Nakada, S., (1991) Magmatic processes in titanite-bearing dacites, central Andes of Chile and Bolivia. American Mineralogist 76, 548 - 560.
[35]. Nandy J, Dey S and Heilimo E (2019) Neoarchaean magmatism through arc and lithosphere melting: evidence from Eastern Dharwar Craton; Geol. J. https://doi.org/10.1002/gj.3498.
[36]. Naqvi S M and Rogers J J W (1987) Precambrian Geology of India; Oxford University Press, New York.
[37]. Narshimha Ch, U.V.B. Reddy, K. Praveen, S. Ramesh (2020) Geochemistry data of the Nadergul granodiorite of the late archean hyderabad granite batholith, part of Eastern Dharwar Craton, India; implications for composition of the lower continental crust. Vol. 31, 2020, 105768. https://doi.org/10.1016/j.dib.2020.105768.
[38]. Pahari A ,Prasanth P, Devleena M Tiwari, Manikyamba C, and K S V Subramanyam (2020) Subduction–collision processes and crustal growth in eastern Dharwar Craton: Evidence from petrochemical studies of Hyderabad granites. J. Earth Syst. Sci. (2020)129 32. https://doi.org/10.1007/s12040-019-1296-1.
[39]. Pahari A, Tang L, Manikyamba C, Santosh M, Subramanyam K S V and Ganguly S (2019) Meso-Neoarchean magmatism and episodic crustal growth in the Kudremukh–Agumbe granite-greenstone belt, Western Dharwar Craton, India; Precamb. Res. 323 16–54.
[40]. Pandey O P, Agrawal P K and Chetty T R K (2002) Unusuallithospheric structure beneath the Hyderabad granitic region, eastern Dharwar craton, south India; Phys. EarthPlanet. Int. 130 59–69.
[41]. Peruginia D, Luca Valentini and Giampiero Poli (2007) Insights into magma chamber processes from the analysis of size distribution of enclaves in lava flows: A case study from Volcano Island (Southern Italy). Journal of Volcanology and Geothermal Research 166, 193-203.

[42]. Peucat J J, Mahabaleswar B and Jayananda M (1993) Age ofyounger tonalitic magmatism and granulitic metamorphismin the south Indian transition zone (Krishnagiri area):Comparison with older peninsular gneisses from theGorur–Hassan area; J. Metamophr. Geol. 11 879–888.
[43]. Poli, G., Perugini, D., (2002) Strange attractors in magmas: evidence from lava flows. Lithos 65, 287–297.
[44]. Praveen K, Anjaneyulu M, Narshimha C and Reddy U V B (2018) Petrology and geochemistry data of the precambrian granitoids from the Hyderabad area, part of Eastern Dharwar Craton, Telangana state, India; Data in Brief 21 1909–1917.
[45]. Radhakrishna T, Balasubramonian G, Joseph M and Krishnendu N R (2004) Mantle processes and geodynamics: Inferences from maBc dykes of south India; Earth System Science and Natural Resources Management, CESS Silver Jubilee Compendium, pp. 3–25.
[46]. Ramakrishnan M and Swaminath J S (1981) Early Precambrian supracrustals of southern Karnataka; Vol. 112, Geol. Surv. India, Bengaluru.
[47]. Sarvothaman H (2001) Archean high-Mg granitoids of mantleorigin in the Eastern Dharwar Craton of Andhra Pradesh;J. Geol. Soc. India 58 261–268.
[48]. Shukla S and Ram Mohan M (2019) Magma mixing in Neoarchean granite from Nalgonda region, Eastern Dharwar Craton, India: Morphological, mineralogical and geochemical evidences; J. Earth Syst. Sci. 128 71.
[49]. Singh A P, Kumar V V and Mishra D C (2004) Subsurfacegeometry of Hyderabad granite pluton from gravity and magnetic anomalies and its role in the seismicity around Hyderabad; Curr. Sci. 86 580–586.
[50]. Smithies R H, Champion D C and Van Kranendonk M J (2009) Formation of Paleoarchean continental crust through intracrustal melting of enriched basalt; Earth Planet. Sci. Lett. 281 298–306.
[51]. Swami Nath J and Ramakrishnan M (eds) (1981) Early Precambrian supracrustals of southern Karnataka; Geol. Surv. India Memoir 112, 352.
[52]. Vernon RH (1984) Microgranitoid enclaves: Globules of hybrid magma quenched in a plutonic environment. Nature 304, 438-439.
[53]. Wiebe , R.A. (1994) Silicic magma chambers a traps for basaltic magmas: The Cadillac mountain intrusive complex, Mount Desert island, Maine. Jour. Geol., v.102, pp.423-427.

Sl. No	1	2	3	4	5	6	7	8	9	10	11	12	13	14	15	16	17	18	19	20	21
Sample	HG-E-01	HG-E-02	HG-E-03	HG-E-04	HG-E-05	HG-E-06	HG-E-07	HG-E-08	HG-E-09	HG-E-10	HG-E-11	HG-E-12	HG-E-13	HG-E-14	HG-E-15	HG-E-16	HG-E-17	HG-E-18	HG-E-19	HG-E-20	HG-E-21
Major elements (Wt %)																					
SiO2	45.42	52.82	52.21	52.99	49.21	52.97	50.94	50.77	53.58	50.00	46.96	49.60	50.92	50.68	50.23	50.73	50.14	50.58	51.01	50.19	50.22
Al2O3	11.46	9.19	9.10	11.76	14.33	9.14	11.66	11.49	10.91	12.71	11.83	12.72	10.80	6.01	11.94	12.32	12.78	12.31	12.13	13.08	11.93
Fe2O3	11.40	12.66	12.25	12.26	12.29	12.23	12.23	12.27	12.99	12.48	11.02	12.52	12.39	12.42	12.45	12.40	12.42	12.39	12.43	12.30	12.46
MnO	0.26	0.20	0.08	0.04	0.17	0.32	0.23	0.19	0.11	0.15	0.42	0.21	0.21	0.26	0.19	0.12	0.16	0.19	0.23	0.24	0.19
MgO	10.74	8.23	4.07	2.79	6.52	8.45	8.03	5.10	2.48	4.60	10.42	5.99	10.5	18.53	9.55	5.34	6.52	6.70	6.66	7.44	9.56

CaO	5.81	5.86	5.45	6.53	4.89	8.14	5.07	5.64	7.06	6.25	3.64	6.01	15.30	5.51	5.78	5.74	5.39	6.21	6.19	6.15	5.79
Na2O	1.26	1.70	9.39	9.88	6.70	4.38	5.31	9.56	8.17	8.05	1.19	8.36	4.59	1.86	5.85	8.66	7.89	8.38	8.46	7.35	5.86
K2O	3.23	4.60	4.28	2.54	2.87	1.48	4.00	2.32	1.98	2.55	5.92	1.68	2.83	2.52	2.10	2.32	2.08	1.70	1.53	1.94	2.10
TiO2	7.10	1.25	0.54	0.27	0.99	0.59	0.66	0.71	0.18	0.99	4.67	0.93	0.64	0.52	0.57	0.73	0.79	0.88	0.72	0.60	0.55
P2O5	2.99	0.01	0.03	0.02	0.31	0.03	0.07	0.17	0.01	0.23	2.41	0.31	0.06	0.02	0.07	0.19	0.26	0.18	0.11	0.07	0.07
LOI	0.19	1.50	1.44	0.64	0.74	0.63	1.03	0.80	1.32	0.95	1.01	0.79	1.00	1.10	0.89	0.47	0.61	0.72	0.53	0.76	0.89
Sum	99.86	98.02	98.84	99.71	99.01	98.37	99.23	99.02	98.78	98.94	99.49	99.12	99.25	99.42	99.63	99.02	99.03	100.24	100.01	100.12	99.63
Na2O+K20	100.05	99.52	100.28	100.35	99.75	99.00	100.26	99.82	100.10	99.89	100.50	99.91	100.25	100.52	100.52	99.49	99.64	100.96	100.54	100.88	100.52
Trace elements (ppm)																					
Sc	80.86	64.18	15.06	4.25	23.81	53.02	14.82	18.05	4.25	8.06	62.64	23.34	20.50	26.49	21.35	12.97	14.86	24.74	17.12	22.31	21.28
V	805.27	181.82	67.47	28.91	190.80	337.68	114.58	147.04	26.64	109.35	303.43	173.13	133.00	133.59	146.90	114.57	158.07	135.31	143.93	137.95	134.97
Cr	204.90	519.71	239.42	200.58	126.24	295.83	325.73	114.93	284.11	219.44	73.20	162.99	839.86	1602.94	639.08	164.82	193.51	212.05	130.24	176.30	172.63
Co	54.13	30.57	13.59	5.81	25.00	50.06	28.61	18.45	61.53	17.12	42.31	28.92	35.61	62.26	33.97	21.95	25.37	28.86	29.45	29.50	28.79
Ni	66.80	55.53	34.57	30.57	41.47	65.51	108.38	27.14	26.83	35.42	42.83	53.09	198.04	490.49	137.84	49.86	52.15	83.16	64.38	77.39	77.31
Cu	23.05	41.53	44.48	19.79	47.13	73.12	33.39	20.35	321.4	30.88	8.65	89.18	18.60	9.24	31.08	144.3	151.0	106.2	36.44	15.99	14.07

									4							0	4	0			
		1				1	3						1							1	
		4	9	6		6	7	8	7	9		9	4		7	8	7	6	9	4	7
	18	6.	0.	3.	89	2.	2.	0.	4.	0.	24	2.	7.	13	7.	0.	8.	4.	1.	1.	9.
	0.	0	7	1	.5	7	6	2	7	7	4.	1	7	7.	1	1	0	6	1	6	6
Zn	20	6	8	2	3	5	4	8	6	1	88	8	1	69	2	6	7	9	6	3	9
		2	2	1		2	1	2	2	2		2	1		1	2	2	2	2	2	2
	41	4.	2.	8.	22	0.	8.	5.	0.	7.	55	9.	6.	11	7.	5.	5.	3.	1.	1.	0.
	.1	3	7	6	.7	8	9	0	0	0	.8	0	7	.9	4	4	0	6	4	1	8
Ga	4	5	0	1	5	0	1	6	3	4	5	1	0	5	8	9	4	1	1	9	8
		3	1	1			4	2		3		1	1		1	1	1				
		6	6	2		9	4	2	8	5	13	9	5		4	0	0	7	5	5	5
	10	8.	4.	7.	12	1.	3.	7.	4.	9.	90	2.	6.	22	6.	8.	5.	9.	4.	6.	6.
	7.	4	9	5	4.	4	8	4	5	2	.1	1	1	9.	9	8	1	5	2	7	3
Rb	72	8	6	2	50	9	3	8	7	2	6	5	6	48	6	2	7	8	2	2	8
		2	4	1		1	3	2	1	2		3	3		5	4	4	3	6	4	4
		3	1	6		5	3	6	3	3		9	9		0	6	9	8	5	6	6
	17	6.	6.	9.	42	5.	8.	7.	5.	8.	86	3.	3.	11	5.	4.	6.	1.	2.	8.	4.
	0.	0	9	7	4.	1	3	6	9	5	.4	7	4	8.	0	8	1	4	4	7	2
Sr	82	9	8	9	73	1	3	0	9	9	7	7	0	96	5	0	3	2	1	8	7
		1																			
		4	2	1		7	2	5	1	9		9	2		2	2	2	5	2	2	2
	66	5.	8.	7.	48	3.	3.	4.	4.	3.	23	8.	9.	20	1.	1.	9.	8.	1.	6.	5.
	2.	3	9	2	.7	0	5	2	6	3	4.	1	0	.4	0	7	8	9	5	3	6
Y	10	3	0	2	4	2	9	6	2	1	19	1	2	4	7	4	1	5	3	3	4
		3	1	1					3	4		2	1			1	1	2		1	1
	64	3	9	4		3	9	9	1	2	53	0	6		9	8	8	0	9	1	0
	79	6.	5.	1.	47	7.	2.	5.	4.	8.	92	1.	8.	11	2.	5.	9.	1.	9.	6.	7.
	.6	8	8	6	4.	7	7	6	1	5	.7	7	3	3.	7	0	7	3	1	5	8
Zr	4	6	0	9	28	2	2	6	5	1	5	7	6	79	0	3	5	2	4	7	2
		2		1		1	1	2		5		3				1	1	1			
	13	0.	9.	1.	28	3.	0.	1.	7.	1.	28	0.	9.	12	6.	4.	8.	7.	6.	8.	8.
	5.	4	7	3	.5	2	4	4	7	5	8.	4	3	.4	3	0	7	2	0	4	2
Nb	03	0	3	8	8	5	6	5	1	9	92	5	8	6	8	6	7	2	7	9	3
		2.	0.	0.		1.	3.	2.	2.	4.	23	2.	1.		1.	0.	0.	0.	0.	0.	0.
	1.	4	3	4	1.	7	8	3	3	4	.0	2	8	5.	3	5	6	5	5	4	4
Cs	19	8	3	7	04	3	5	2	9	9	3	5	6	03	3	4	7	3	0	6	4
		2	6	3			3	1	1	2		1	4		3	2	2	3	2	2	2
		4	5	2	11	7	3	5	8	4		2	1		4	7	8	4	2	6	4
	33	0.	0.	3.	65	4.	9.	2.	8.	5.	15	7.	2.	17	0.	2.	8.	5.	1.	4.	5.
	6.	6	2	3	.9	4	3	1	2	1	0.	9	7	8.	7	0	8	2	5	5	0
Ba	94	4	3	7	4	4	8	0	1	2	69	9	3	96	6	1	6	3	2	3	6
			1																		
	29	7	3	5		1	3	5	5	8		6	3		3	5	6	8	2	2	2
	59	8.	5.	9.	10	3.	2.	3.	3.	2.	57	4.	4.	35	0.	2.	7.	9.	1.	1.	0.
	.2	2	0	1	2.	7	1	4	0	1	9.	6	1	.8	8	4	0	9	5	5	8
La	2	4	5	5	85	0	9	3	2	3	52	2	3	1	6	3	9	4	7	1	7
		1	2	1				1		1		1				1	1	1			
	57	7	4	0		4	6	2	9	9	12	6	8		6	1	4	8	4	4	4
	07	5.	8.	7.	21	5.	9.	4.	3.	6.	22	2.	6.	87	9.	2.	7.	6.	6.	7.	6.
	.4	4	5	1	8.	7	9	3	2	9	.3	9	3	.9	6	7	7	8	5	9	6
Ce	9	5	6	2	32	0	8	5	4	5	9	0	1	4	7	0	4	5	7	3	9
		2	2	1				1		2		2	1			1	1	2			
	60	2.	4.	0.	24	7.	8.	5.	8.	5.	11	2.	1.	11	8.	3.	7.	1.	5.	6.	5.
	6.	7	2	5	.8	1	7	3	9	1	0.	2	4	.4	4	2	6	0	9	0	8
Pr	56	2	7	8	6	3	4	0	3	8	14	5	3	1	8	5	8	6	2	4	8
	17	9	7	3	93	3	3	5	2	1	35	9	4	46	3	5	6	7	2	2	2
	95	6.	8.	4.	.5	2.	5.	9.	8.	0	5.	5.	6.	.5	2.	1.	9.	8.	4.	5.	4.
Nd	.4	5	7	4	5	8	1	1	3	2.	56	1	7	0	9	8	6	9	8	2	5

	4	9	1	0		2	2	5	5	5		7	6		4	4	9	3	8	4	6
										6											
		2	1			1		1		2		2					1	1			
	26	6.	2.	5.	16	0.	7.	3.	4.	2.	58	2.	9.		6.	8.	2.	6.	5.	5.	5.
	9.	8	8	3	.6	4	0	1	7	5	.9	8	3	8.	2	9	6	0	3	6	4
Sm	39	9	5	3	6	1	6	5	2	8	4	2	8	48	0	4	0	6	2	4	5
		1.	1.	1.		1.	1.	1.	0.	2.		1.	1.		1.	1.	2.	1.	1.	1.	1.
	6.	5	5	0	3.	2	5	0	7	4	2.	8	9	1.	7	6	2	6	4	3	2
Eu	97	4	7	1	24	8	0	7	6	0	06	1	1	79	3	2	6	7	8	0	9
		2				1		1		1		1						1			
	18	6.	9.	4.	12	1.	5.	1.	3.	8.	45	9.	7.		4.	6.	9.	3.	4.	5.	4.
	9.	6	6	1	.7	0	4	2	5	5	.7	0	1	6.	8	5	2	7	6	0	8
Gd	76	8	9	6	6	1	3	0	9	2	7	2	9	50	5	3	3	9	0	6	6
	23	4.	1.	0.		1.	0.	1.	0.	2.		2.	0.		0.	0.	1.	1.	0.	0.	0.
	.6	6	2	5	1.	8	7	6	4	6	6.	7	9	0.	6	7	0	9	6	7	7
Tb	3	4	5	3	60	8	1	2	4	5	18	4	2	78	5	6	6	3	4	4	2
		2				1				1		1						1			
	12	8.	6.	2.		1.	3.	9.	2.	4.	34	5.	4.		3.	3.	5.	0.	3.	4.	4.
	0.	3	3	8	8.	9	7	1	3	8	.2	5	8	3.	5	8	3	5	6	4	2
Dy	99	5	8	6	34	0	3	0	1	3	3	4	2	89	4	4	3	4	1	0	1
	22	5.	1.	0.		2.	0.	1.	0.	2.		3.	0.		0.	0.	0.	2.	0.	0.	0.
	.0	5	1	5	1.	4	7	8	4	9	7.	1	9	0.	7	7	9	0	7	9	8
Ho	0	4	3	9	59	3	3	1	8	5	11	1	4	73	3	2	9	3	3	1	9
		1																			
	51	3.	2.	1.		6.	1.	4.	1.	7.	19	8.	2.		1.	1.	2.	5.	1.	2.	2.
	.5	1	5	4	4.	4	9	7	2	5	.5	2	4	1.	9	9	5	1	9	4	3
Er	9	0	3	7	09	6	3	4	9	1	5	5	2	78	0	2	3	3	5	3	8
		1.	0.	0.		0.	0.	0.	0.	1.		1.	0.		0.	0.	0.	0.	0.	0.	0.
	6.	5	2	2	0.	9	2	6	2	0	2.	1	3	0.	2	2	3	6	2	3	3
Tm	36	8	9	0	60	4	9	5	0	2	97	7	6	25	9	7	6	8	9	5	5
	38	8.	1.	1.		6.	1.	4.	1.	5.	19	7.	2.		1.	1.	2.	4.	1.	2.	2.
	.1	0	6	1	3.	0	8	0	4	8	.9	1	3	1.	8	8	3	0	9	2	2
Yb	2	0	3	4	92	1	2	1	2	9	1	4	5	60	0	1	5	8	5	5	0
		0.	0.	0.		0.	0.	0.	0.	0.		0.	0.		0.	0.	0.	0.	0.	0.	0.
	5.	9	2	1	0.	8	2	5	2	7	3.	9	3	0.	2	2	3	5	2	3	3
Lu	51	1	1	6	59	1	6	4	3	6	10	6	4	23	7	8	7	7	9	3	2
	15	8.	4.	4.	10	1.	2.	2.	7.	9.	13	4.	4.		2.	4.	4.	5.	2.	2.	2.
	0.	0	7	0	.4	4	2	5	8	6	0.	8	1	3.	4	4	7	1	6	9	7
Hf	71	9	1	0	8	1	9	5	8	7	80	6	0	01	0	6	1	3	3	4	9
		0.	0.	0.		1.	0.	0.	0.	4.	18	1.	0.		0.	0.	1.	1.	0.	0.	0.
	7.	9	3	5	1.	4	7	9	7	6	.9	7	7	0.	3	7	4	0	7	9	8
Ta	09	4	6	7	22	6	8	8	5	4	3	9	3	84	9	4	0	4	2	4	8
	61	5.	8.	8.		4.	9.	4.	6.	6.	71	5.	5.		5.	6.	5.	6.	5.	6.	5.
	.1	7	9	8	8.	2	1	5	5	1	.9	1	1	3.	9	3	8	5	5	6	2
Pb	4	0	3	0	15	3	1	6	8	5	9	9	2	73	9	4	8	1	4	5	3
	17	1	3	3					3	3	21						1	2			
	20	9.	1.	8.	42	2.	4.	4.	1.	0.	91	2.	7.		5.	8.	0.	9.	3.	3.	3.
	.1	6	2	3	.3	3	5	6	9	4	.3	7	4	6.	5	1	0	9	5	6	1
Th	1	9	8	7	1	7	6	2	4	5	2	8	2	85	5	7	4	1	7	6	7
									3	1											
	40	2.	1.	4.		2.	2.	8.	3.	0.	31	0.	1.		0.	1.	1.	4.	1.	2.	2.
	.5	0	4	0	5.	2	3	2	7	6	2.	9	0	1.	7	0	9	0	9	4	2
U	4	0	6	1	34	3	5	8	0	0	57	9	7	61	4	7	9	4	4	9	8

S Ramesh, et. al. "Characterization of microgranular enclaves of Hyderabad batholith, Eastern Dharwar Craton, India." *International Journal of Engineering Science Invention (IJESI)*, Vol. 11(01), 2022, PP 01-14. Journal DOI- 10.35629/6734